Chapter 1

Introduction

1.1 Why Pursue Non-Gaussianity in CMB?

Modern understanding to emergence of inhomogeneity in the universe through the cosmic history is outstanding; the inhomogeneity is *quantum* in origin. Then, it becomes classical through its evolution, producing fluctuations in the *cosmic microwave background* (CMB) radiation, and creating complex structures, such as galaxies, seen in the present universe.

A theory of early universe, the cosmic *inflation* (Guth, 1981; Sato, 1981; Albrecht and Steinhardt, 1982; Linde, 1982), has predicted the emergence of the quantum fluctuations in early universe. Inflation not only resolves several serious issues in the old Big-Bang cosmology, but also gives a mechanism to produce inhomogeneity in the universe, and makes specific testable predictions for the global structure and the inhomogeneity in the universe (Guth and Pi, 1982; Hawking, 1982; Starobinsky, 1982; Bardeen et al., 1983). The predictions may concisely be summarized as follows:

(a) The observable universe is spatially flat.

(b) The observable universe is homogeneous and isotropic on large angular scales, apart from tiny fluctuations.

(c) The primordial inhomogeneity has a specific spatial pattern, so-called the scale-invariant fluctuation.

(d) Statistics of the primordial inhomogeneity obey *Gaussian statistics*.

All these predictions but (d) have passed challenging observations. Among those observations, the most firm evidence supporting the predictions has come from measurement of the angular distribution of CMB. Being the oldest observable object in the universe, CMB is the best clue to early universe.

Observed isotropy of CMB with 0.001% accuracy* supports the prediction (b) (Mather et al., 1990; Smoot et al., 1992). The measured angular distribution of the CMB anisotropy, 0.001%

*Apart from anisotropies due to the local motion of the Earth, which is of order 0.1% (Smoot et al., 1991).

inhomogeneity, supports the primordial fluctuation distribution being consistent with the prediction (c) in the flat universe, the prediction (a) (Bennett et al., 1996; Miller et al., 1999; de Bernadis et al., 2000; Hanany et al., 2000).

Using various statistical techniques, many authors have attempted to test the prediction (d), the Gaussianity of the primordial inhomogeneity, using the CMB anisotropy on large angular scales ($\sim 7^\circ$) (Kogut et al., 1996b; Ferreira et al., 1998; Pando et al., 1998; Bromley and Tegmark, 1999; Banday et al., 2000; Mukherjee et al., 2000; Magueijo, 2000; Sandvik and Magueijo, 2000; Barreiro et al., 2000), on intermediate scales ($\sim 1^\circ$) (Park et al., 2001), and on small scales ($\sim 10'$) (Wu et al., 2001).

In contrast to the predictions (a)–(c) for which the observations suggest no controversy, previous work on searching for non-Gaussian CMB anisotropies has come to different conclusions from one another: some do claim detection (Ferreira et al., 1998; Pando et al., 1998; Magueijo, 2000), and the others do not (Kogut et al., 1996b; Sandvik and Magueijo, 2000; Barreiro et al., 2000; Park et al., 2001; Wu et al., 2001). Furthermore, Bromley and Tegmark (1999) and Banday et al. (2000) claim the non-Gaussian signal of Ferreira et al. (1998) to be non-cosmological in origin. Mukherjee et al. (2000) revise the conclusion of Pando et al. (1998) by addressing ambiguity in their method, from which the conclusion crucially depends upon an orientation of the data on the sky, and show no evidence for the non-Gaussianity. The existence of non-Gaussianity in CMB is controversial.

Since non-Gaussianity has infinite degrees of freedom, testing a Gaussian hypothesis is difficult; one statistical method showing CMB *consistent* with Gaussian does not mean CMB being *really* Gaussian. In this sense, different statistical methods can come to different conclusions. In addition to the difficulty, cosmological non-Gaussianity is hard to measure. Instrumental and environmental effects in observations easily produce spurious non-Gaussian signals. Astronomical microwave sources such as interstellar dust emissions also produce strong non-Gaussian fluctuations on the sky. Hence, we must be as careful as possible when searching for cosmological non-Gaussianity.

Pursuit of cosmological non-Gaussianity in CMB is a challenging test of inflation, the origin of inhomogeneity in the universe. In this dissertation, we present theoretical and observational studies of the CMB non-Gaussianity. Our primary goal is to test inflation with non-Gaussian CMB fluctuations.

As a statistical tool of searching for non-Gaussianity, we use the angular three- and four-point correlation functions in harmonic space, the *angular bispectrum* and *trispectrum*, which are sensitive to weakly non-Gaussian fluctuations. An advantage of these angular n-point harmonic spectra over other statistics is that they are predictable from not only inflation, but also secondary sources in the low-redshift universe (the Sunyaev–Zel'dovich effect, weak gravitational lensing effect, and so on), extragalactic foreground emissions, global topology of the universe, and so on. When we fit those predictions to the measured spectra, the predictions become "matched filters" for detecting weak non-Gaussianity in the data, and much more powerful than just a null test of Gaussianity.

This dissertation is organized as follows. The rest of this chapter will overview what the CMB sky looks like, and the previous study of CMB non-Gaussianity, followed by a heuristic description of non-Gaussian fluctuation production in inflation.

In chapter 2, we go through primordial fluctuation generation mechanism in inflation, and investigate how non-linear curvature perturbations are generated and propagated through the CMB anisotropy. We present a possible quantum-to-classical transition mechanism of the quantum fluctuations on super horizon scales.

In chapter 3, we study statistical properties of the angular n-point harmonic spectrum for $n = 2$ (power spectrum), 3 (bispectrum), and 4 (trispectrum). We present practical methods of measuring the angular bispectrum and trispectrum from observational data with many pixels.

In chapter 4, we make theoretical predictions for the CMB angular bispectrum, which include primary contribution from inflation, secondary contribution from the Sunyaev–Zel'dovich effect and the weak-lensing effect, and foreground contribution from extragalactic radio and infrared astronomical sources. We estimate signal-to-noise ratios of detecting each contribution with CMB experiments, further discussing how well we can measure each contribution separately.

In chapter 5, we measure the angular bispectrum on the *COBE* DMR four-year data, testing Gaussianity of the data. By fitting the theoretical prediction for the primary bispectrum to the data, we constrain non-linearity in inflation; also fitting foreground bispectra from interstellar microwave emissions takes into account the effect of non-Gaussian interstellar dust and synchrotron emissions at high Galactic latitude.

In chapter 6, we measure the angular trispectrum on the DMR data, further testing Gaussianity of the data.

1.2 Inhomogeneity in Microwave Sky

The cosmic microwave background radiation (CMB) is the isotropic microwave radiation filling the sky. The temperature is precisely measured to be 2.73 K (Mather et al., 1990), and the peak intensity at $\nu = 160$ GHz ($\lambda = 1.9$ mm) is 370 MJy str^{-1}. What if subtracting this mean radiation from the sky, what are we left with, completely dark, literally nothing?

1.2.1 *COBE* DMR sky maps

The Differential Microwave Radiometer (DMR) mounted on the *Cosmic Background Explorer* (*COBE*), the satellite for full sky measurement of CMB launched by NASA in 1989, has revealed that what we are left with is the tiny inhomogeneity; the r.m.s. amplitude is about 30 μK (Smoot et al., 1992), 0.001% of the mean temperature.

Various statistical analyses on the DMR sky maps have shown the angular distribution of the CMB anisotropy remarkably consistent with the scale-invariant fluctuation, the prediction of inflation (Bennett et al., 1996; Górski et al., 1996; Hinshaw et al., 1996; Wright et al., 1996). The scale-invariant fluctuation implies that the r.m.s. amplitude of the CMB anisotropy is nearly independent of angular scales. DMR has measured 35 μK r.m.s. fluctuations on 7° scale, 29 μK on 10° scale (Banday et al., 1997).

DMR comprises 3 dual-horn antennas working at 31.5, 53, and 90 GHz. The combination of 53 and 90 GHz maps gives the most sensitive sky map to CMB, while 31.5 GHz map is twice as

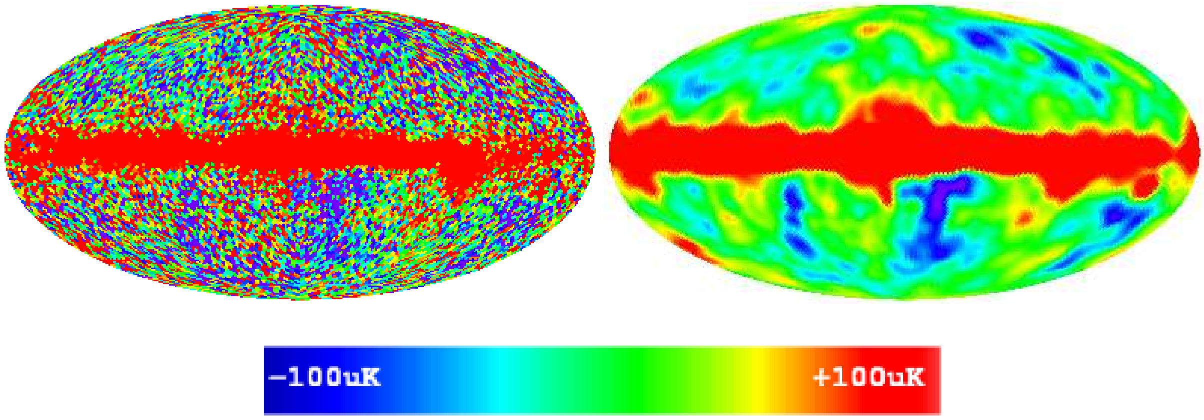

Figure 1.1: *COBE* DMR Sky Map

COBE DMR four-year 53 + 90 GHz sky map in Galactic projection, using the HEALPix pixelization (Górski et al., 1998) with $1^\circ\!.83$ pixel size, leaving 12,288 pixels. The left is the raw map, while the right map has been smoothed with a 7° FWHM Gaussian.

noisier as the other channels. Figure 1.1 shows the combined DMR full sky map. The left shows the raw map in which the instrumental noise dominates appearance of the map; the right shows the smoothed map with the DMR beam in which the instrumental noise is filtered out, giving better appearance of CMB signals. The mean signal-to-noise ratio of hot and cold spots in the smoothed map is 2, while a few prominent spots have 3 to 4. Hence, we cannot say much about structures of the CMB anisotropy relying on the map basis; however, we can do say on the statistical basis.

Statistically, structures in the DMR map are inconsistent with pure instrumental noise; on the contrary, the structure has a distinct angular correlation pattern represented by the scale-invariant fluctuation. To quantify this, it is useful to calculate the *angular power spectrum*, C_l, the harmonic transform of the angular two-point correlation function, which measures how much fluctuation power exists on a given angular scale, $\theta \sim \pi/l$. Figure 1.2 plots the measured C_l on the DMR map. What is actually plotted is $l(l+1)C_l/2\pi$, roughly mean squares of fluctuations at l. The scale-invariant fluctuation implies $C_l \propto [l(l+1)]^{-1}$ (Peebles, 1982), and hence $l(l+1)C_l$ remains constant (solid line), so do the data points in the figure; the data points fit the inflation's prediction well. The dashed line shows a more accurate prediction, taking into account the effects of general relativistic photon-baryon fluid dynamics before the decoupling as well as of time evolution of gravitational potential field after the decoupling. The agreement with the data becomes better, further confirming that the DMR angular power spectrum is consistent with inflation.

Gaussianity of the DMR data has been tested with various statistical methods (Kogut et al., 1996b; Ferreira et al., 1998; Pando et al., 1998; Bromley and Tegmark, 1999; Banday et al., 2000; Mukherjee et al., 2000; Magueijo, 2000; Sandvik and Magueijo, 2000; Barreiro et al., 2000). Ferreira et al. (1998) and Magueijo (2000) claim positive detection of non-Gaussian signals using the angular bispectrum, and Pando et al. (1998) claim detection using the wavelet analysis. The latter non-

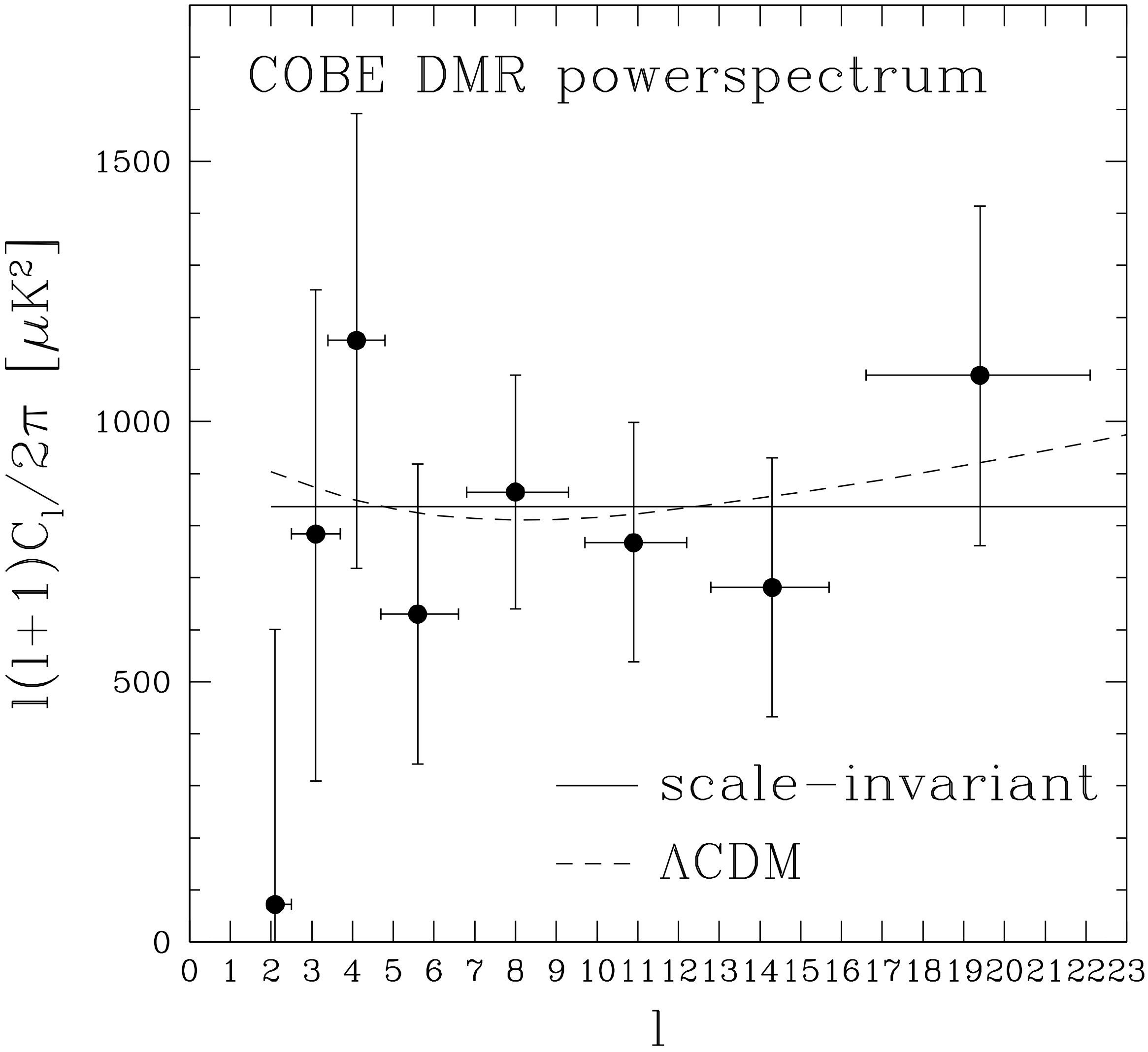

Figure 1.2: *COBE* DMR Angular Power Spectrum

The CMB angular power spectrum, C_l, measured on the *COBE* DMR four-year map. The plotted quantity, $l(l + 1)C_l/(2\pi)$, represents the r.m.s. amplitude of fluctuations at a given angular scale, l. The data points (filled circles) are uncorrelated with each other (Tegmark and Hamilton, 1997). The solid line shows the scale-invariant power spectrum, $l(l + 1)C_l$ = constant, while the dashed line shows a ΛCDM spectrum.

Gaussian signal has appeared to be less significant than they claim, as it disappears when the DMR map is rotated by 180° (Mukherjee et al., 2000; Barreiro et al., 2000). For the former two bispectrum analyses, Bromley and Tegmark (1999) and Banday et al. (2000) claim that the Ferreira et al. (1998)'s signal is non-cosmological, but their claims do not account for the Magueijo (2000)'s signal. In this thesis, we will argue that the reported non-Gaussian signals are not a matter of origin, but statistical fluctuations.

1.2.2 Post-*COBE* era

After the discovery of *COBE*, pursuit of the CMB anisotropy has been oriented toward measurement of the angular power spectrum, C_l, on smaller angular scales, i.e., larger l. Particularly, many efforts have been made to measure C_l at $l \sim 200$ ($\theta \sim 1^\circ$), where inflation predicts a prominent peak in $l(l+1)C_l$ as a consequence of flatness of the universe, the prediction of inflation (Kamionkowski et al., 1994).

By early 2000, there has been strong evidence for the peak (Miller et al., 1999); in the end of 2000, *BOOMERanG* and *MAXIMA*, balloon-borne CMB experiments, have detected the peak (de Bernadis et al., 2000; Hanany et al., 2000), further supporting inflation. Figure 1.3 compares the data from three experiments, which probe different angular scales from one another, with a prediction from inflation. The agreement between the data and the prediction is outstanding.

Measurement of C_l so far, however, has assumed CMB Gaussian. If CMB is not Gaussian, then the measured C_l is biased. Moreover, when we fit the measured C_l to a theoretical C_l, we need to know the covariance matrix of C_l. Since the covariance matrix of C_l is the four-point harmonic spectrum, the trispectrum, we have to investigate non-Gaussian signals in the trispectrum to construct the covariance matrix accurately.

Even if non-Gaussianity is small, we have to take it into account in analyzing C_l; the next generation satellite experiments, *MAP* and *Planck*, will measure C_l with 1% or better accuracy, and we will use the measured C_l to determine many of cosmological parameters with 10% or better accuracy. Unless non-Gaussian effect is much smaller than the observational uncertainty (who knows?), we have to take the effect into account, to achieve the accurate measurement of the parameters.

The state-of-the-art balloon-borne experiments provide not only C_l, but also high resolution, high signal-to-noise ratio CMB maps. The left of figure 1.4 shows the *BOOMERanG* sky map, which covers roughly 3% of the sky, 1,800 square degrees, with $10'$ ($0\overset{\circ}{.}17$) angular resolution. The high signal-to-noise ratios in the map show the observed structures in the map not instrumental noise, but CMB.

Visually, the CMB anisotropy in the map looks very much Gaussian, implying non-Gaussianity is weak, if any. As yet the *BOOMERanG* team has not performed Gaussianity tests on the data; however, the *MAXIMA* team has done on their data. The *MAXIMA* map covers 124 square degrees of the sky with $10'$ angular resolution, leaving 5,972 pixels. They have found that the one-point probability density distribution function and the Minkowski functionals measured on the map are consistent with Gaussianity.

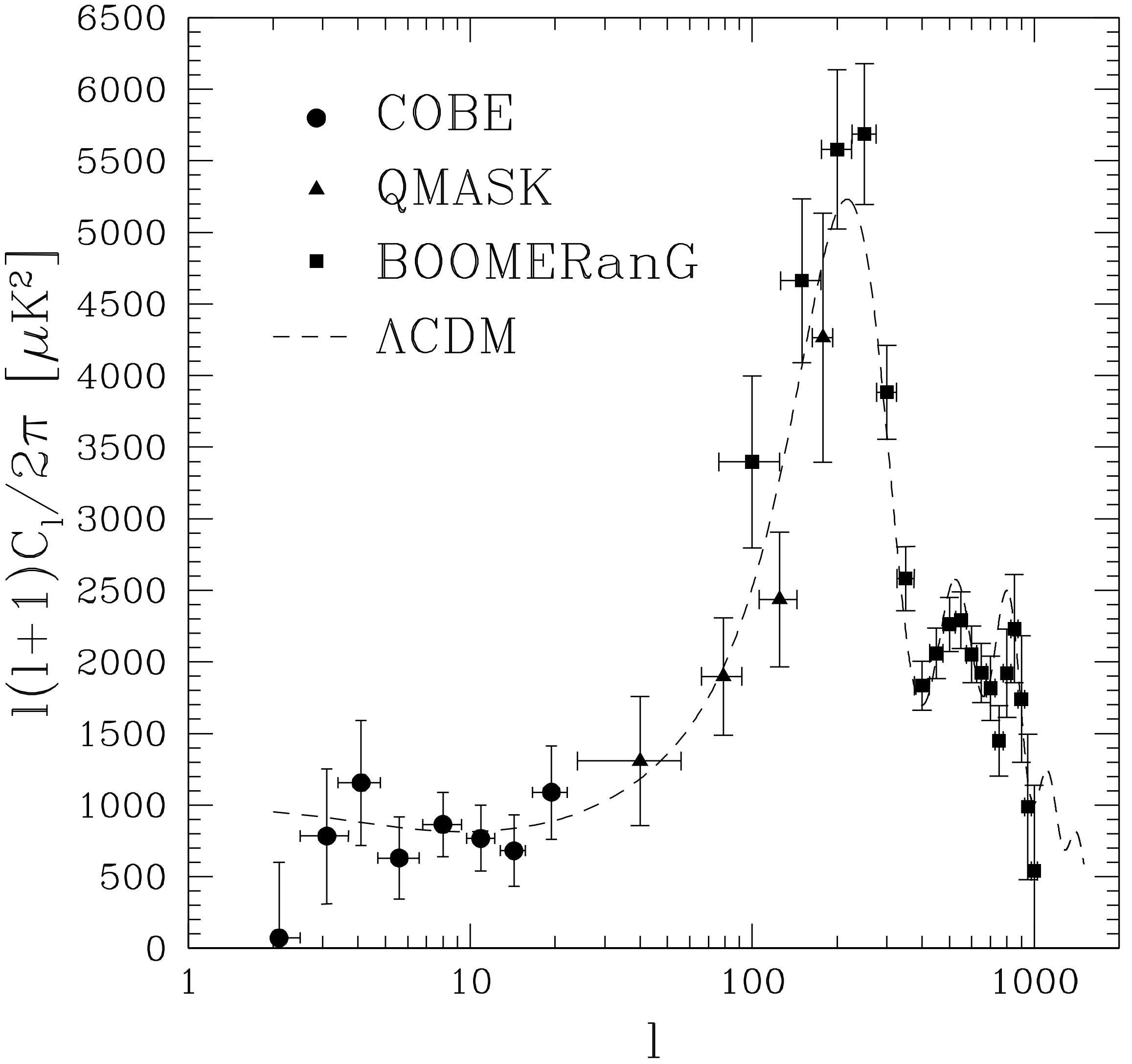

Figure 1.3: *COBE* DMR, *QMASK*, and *BOOMERanG* Angular Power Spectra
The CMB angular power spectrum, measured by the three experiments probing different angular scales. The circles are the *COBE* DMR data (full sky coverage with a Galactic cut, 7° angular resolution), the triangles are the *QMASK* data (648-square-degree sky coverage, 0.°68 angular resolution), and the squares are the *BOOMERanG* data (1,800-square-degree sky coverage, 0.°17 angular resolution). The dashed line shows a prediction of inflation, a ΛCDM spectrum with $\Omega_{\rm m} = 0.3$, $\Omega_\Lambda = 0.7$, $\Omega_{\rm b} = 0.04$, $h = 0.7$, and $n = 0.95$.

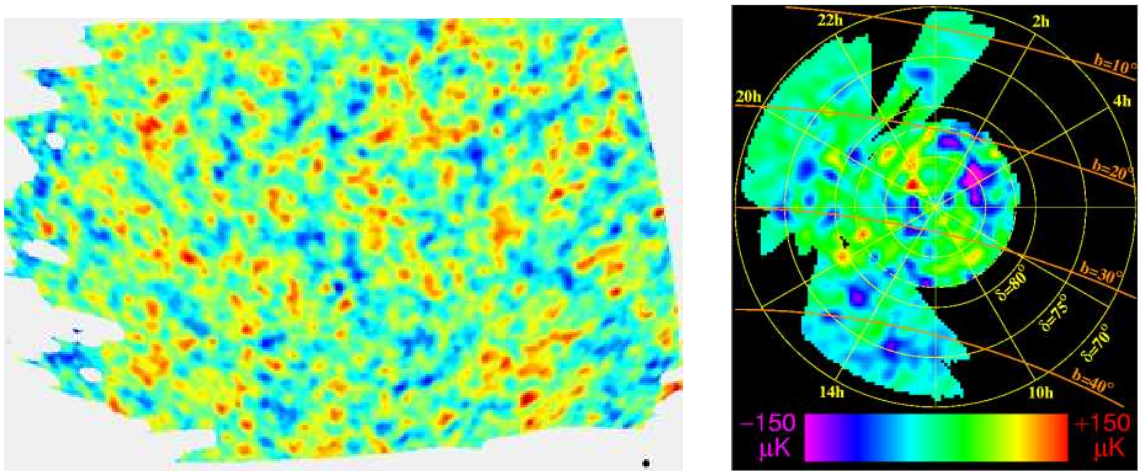

Figure 1.4: Sub-degree CMB Maps: *BOOMERanG* and *QMASK*

The left is the *BOOMERanG* sky map, which covers 3% of the sky, 1,800 square degrees, with $10'$ ($0^\circ\!\!.17$) angular resolution (de Bernadis et al., 2000). The beam size is indicated by the filled circle at the bottom-right corner. The right is the *QMASK* sky map, which covers 648 square degrees of the sky with $0^\circ\!\!.68$ angular resolution (Xu et al., 2001). Both maps have been scaled to match each other in size. The *QMASK* map is one-third of the *BOOMERanG* map.

The genus statistic has been applied to the *QMASK* map (Xu et al., 2001), a high signal-to-noise ratio CMB map combining the balloon-borne *QMAP* (Devlin et al., 1998; Herbig et al., 1998; de Oliveira-Costa et al., 1998) and the ground-based *Saskatoon* experiments (Netterfield et al., 1997), showing the map consistent with Gaussian (Park et al., 2001). The *QMASK* map is shown on the right of figure 1.4, where the size of the map has been scaled to match the *BOOMERanG* map. The *QMASK* map covers 648 square degrees of the sky, one-third of the *BOOMERanG* map, with $0^\circ\!\!.68$ angular resolution, leaving 6,495 pixels.

The number of independent pixels that has been used for Gaussianity tests on the DMR (3,881), *MAXIMA* (5,972), and *QMASK* (6,495) data is similar to each other; although their angular scales are quite different, they have similar power of testing Gaussianity. We will have a significant progress when the *BOOMERanG* data, in which the number of pixels is 57,103, test the Gaussianity.

The just-launched CMB satellite, the *Microwave Anisotropy Probe* (*MAP*), will increase our power of pursuing non-Gaussianity substantially. It will survey the full sky with the angular resolution better than $14'$, and have $\gtrsim 10^6$ pixels. The statistical methods developed in this thesis can readily be applied to the *MAP* data, enabling us to test the Gaussianity with unprecedented sensitivity.

1.3 Non-Gaussian Fluctuations in Inflation

1.3.1 Adiabatic production of non-Gaussian fluctuations

While inflation predicts Gaussian CMB fluctuations to very good accuracy, strictly speaking, non-linearity in inflation produces weakly non-Gaussian fluctuations, which propagates through CMB. Although the exact treatment is complicated, we present a basic idea behind it concisely here (Komatsu and Spergel, 2001b).

The curvature perturbations, Φ, generate the CMB anisotropy, $\Delta T/T$. The linear perturbation theory gives a linear relation between Φ and $\Delta T/T$,

$$\frac{\Delta T}{T} \sim g_{\rm T}\Phi, \tag{1.1}$$

where $g_{\rm T}$ is the radiation transfer function. For temperature fluctuations on super-horizon scales at the decoupling epoch, the Sachs-Wolfe effect (Sachs and Wolfe, 1967) dominates, and $g_{\rm T} = -1/3$ for adiabatic fluctuations. On sub-horizon scales, $g_{\rm T}$ oscillates (acoustic oscillation), and we need to solve the Boltzmann photon transport equations coupled with the Einstein equations for $g_{\rm T}$. It follows from the relation, $\Delta T \propto \Phi$, that ΔT is Gaussian, if Φ is Gaussian. As we will see, non-linearity in inflation makes Φ weakly non-Gaussian.

Even if Φ is Gaussian, $\Delta T/T$ can be non-Gaussian. According to the general relativistic cosmological perturbation theory, there is a non-linear relation between $\Delta T/T$ and Φ:

$$\frac{\Delta T}{T} \sim g_{\rm T}\left(\Phi + f_\Phi \Phi^2\right). \tag{1.2}$$

Here, the second term with a coefficient of order unity, $f_\Phi \sim \mathcal{O}(1)$, is the higher-order correction arising from the second-order perturbation theory (Pyne and Carroll, 1996). It produces non-Gaussian fluctuations; thus, even if Φ is Gaussian, ΔT becomes weakly non-Gaussian.

Is Φ Gaussian? Non-linearity in inflation makes Φ weakly non-Gaussian. By expanding the fluctuation dynamics in inflation up to the second order, we obtain a non-linear relation between Φ and inflaton fluctuations, $\delta\phi$:

$$\Phi \sim m_{\rm pl}^{-1} g_\Phi \left(\delta\phi + m_{\rm pl}^{-1} f_{\delta\phi}\delta\phi^2\right). \tag{1.3}$$

Salopek and Bond (1990) show that this relation is a non-linear solution for curvature perturbations on super horizon scales; the solution gives $g_\Phi \sim \mathcal{O}(10)$ and $f_{\delta\phi} \sim \mathcal{O}(10^{-1})$ for a class of slowly-rolling single-field inflation models.

Quantum fluctuations produce Gaussian $\delta\phi$. If the dynamics of $\delta\phi$ is simple enough to keep itself Gaussian throughout the evolution, then we can stop our consideration here; however, it is not necessarily true. For example, non-trivial interaction terms in the equation of motion for inflaton fields (Falk et al., 1993), or a non-linear coupling between long-wavelength classical fluctuations and short-wavelength quantum fluctuations in the context of stochastic inflation (Starobinsky, 1986; Gangui et al., 1994), can make $\delta\phi$ weakly non-Gaussian, resulting in a non-linear relation between $\delta\phi$ and a Gaussian field, η,

$$\delta\phi \sim g_{\delta\phi}\left(\eta + m_{\rm pl}^{-1} f_\eta \eta^2\right), \tag{1.4}$$

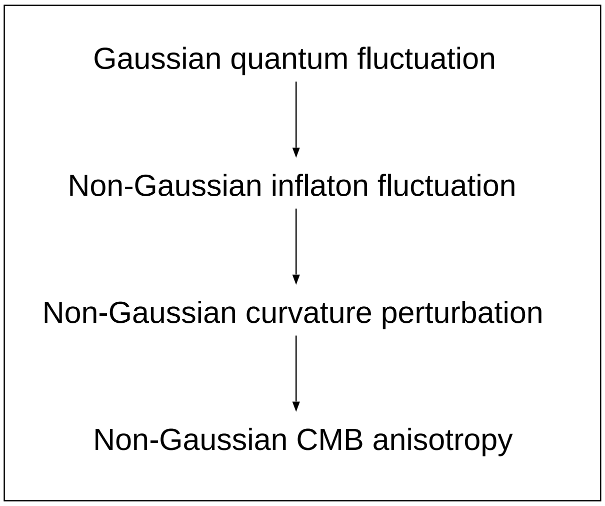

Figure 1.5: Three Steps for Non-Gaussian CMB Anisotropy

Adiabatic generation of non-Gaussian CMB anisotropies. First, inflation generates Gaussian quantum fluctuations, which become non-Gaussian inflaton fluctuations through a non-linear coupling between them (Eq.(1.4)). Then, the inflaton fluctuations become more non-Gaussian curvature perturbations through a non-linear relation between them (Eq.(1.3)). Finally, the curvature perturbations become more non-Gaussian CMB anisotropies through non-linear gravitational effects (Eq.(1.2)).

where η represents initially produced quantum fluctuations, and $g_{\delta\phi} \sim 1$ and $f_\eta \sim \mathcal{O}(10^{-1})$. Figure 1.5 summarizes the above three steps in the opposite order.

Collecting all the above contributions, we obtain a non-linear relationship between $\Delta T/T$ and Φ,

$$\frac{\Delta T}{T} \sim g_{\rm T}\left[\Phi_{\rm L} + \left(f_\Phi + g_\Phi^{-1} f_{\delta\phi} + g_\Phi^{-1} g_{\delta\phi}^{-1} f_\eta\right)\Phi_{\rm L}^2\right], \tag{1.5}$$

where $\Phi_{\rm L} \equiv g_\Phi g_{\delta\phi} m_{\rm pl}^{-1}\eta \sim 10 m_{\rm pl}^{-1}\eta$ is an auxiliary Gaussian curvature perturbation. It may be useful to define a *non-linear coupling parameter*, $f_{\rm NL} = f_\Phi + g_\Phi^{-1} f_{\delta\phi} + g_\Phi^{-1} g_{\delta\phi}^{-1} f_\eta$. The first term in $f_{\rm NL}$, the second order gravity effect $\sim \mathcal{O}(1)$, is dominant compared with the other two terms $\sim \mathcal{O}(10^{-2})$, non-linearity in slow-roll inflation. Note that $f_{\rm NL}$ corresponds to $-\Phi_3/2$ in Gangui et al. (1994) and $-\alpha_\Phi$ in Verde et al. (2000). Using $f_{\rm NL}$, we rewrite equation (1.5) as $\Delta T(\mathbf{x})/T \sim g_{\rm T}\Phi(\mathbf{x})$, where

$$\Phi(\mathbf{x}) = \Phi_{\rm L}(\mathbf{x}) + f_{\rm NL}\left[\Phi_{\rm L}^2(\mathbf{x}) - \left\langle \Phi_{\rm L}^2(\mathbf{x})\right\rangle\right], \tag{1.6}$$

the angular bracket denoting the statistical ensemble average.

To see intuitively what non-Gaussian fluctuations that we have considered here look like, in figure 1.6 we plot one-point probability density distribution function (p.d.f) of the CMB anisotropy. We compare Gaussian p.d.f with non-Gaussian p.d.f of adiabatic fluctuations produced in inflation. The dashed line is Gaussian distribution, i.e., no non-linear perturbations are included ($f_{\rm NL} = 0$).

The solid line includes non-linear coupling of order $f_{\rm NL} = 10^3$, while the dotted line of order $f_{\rm NL} = 10^4$. It follows from the figure that positive $f_{\rm NL}$ gives negatively skewed p.d.f; negative $f_{\rm NL}$ gives positively skewed p.d.f. The larger $|f_{\rm NL}|$ is, the more skewed p.d.f becomes.

We find that $f_{\rm NL} = 10^3$ gives virtually identical p.d.f to the Gaussian p.d.f. In chapter 4, we will show that even with the ideal CMB experiment, we can measure $|f_{\rm NL}|$ no smaller than 60, if we use the skewness of the one-point p.d.f. If we use the bispectrum, however, we can measure as small $|f_{\rm NL}|$ as 3. The bispectrum is thus much more sensitive to the adiabatic non-Gaussianity than the skewness of the one-point p.d.f is. In chapter 5, we will show that the angular bispectrum measured on the *COBE* DMR sky map constrains $|f_{\rm NL}| < 1.6 \times 10^3$. The next generation satellite experiments, *MAP* and *Planck*, will improve the constraint substantially.

Since the minimum $|f_{\rm NL}|$ detectable with CMB experiments is 3, the second order gravity effect, $f_{\rm NL} \sim \mathcal{O}(1)$, will not produce detectable non-Gaussianity in CMB, nor will slow-roll inflation, $f_{\rm NL} \sim \mathcal{O}(10^{-2})$.

Yet, inflation may not be so simple. Any significant deviation from slow-roll, or features in an inflaton potential (Kofman et al., 1991), could produce a bigger $|f_{\rm NL}|$, bigger non-Gaussianity. While we have restricted ourselves to adiabatic fluctuations, the deviation from Gaussianity can be more significant if inflation produces non-negligible isocurvature fluctuations (Linde and Mukhanov, 1997; Bucher and Zhu, 1997; Peebles, 1997). Measurement of non-Gaussian CMB anisotropies thus potentially constrains non-linearity, "slow-rollness", and "adiabaticity" in inflation. In the next subsection, we concisely describe a possible mechanism to produce isocurvature fluctuations in inflation.

1.3.2 Isocurvature fluctuations

Isocurvature fluctuations do not perturb spatial curvature at the initial fluctuation-generation epoch. In inflation, in addition to a scalar field responsible for adiabatic fluctuations, another scalar field, σ, may produce isocurvature density fluctuations with amplitude of $\delta\rho_\sigma/\rho_\sigma \sim H^2/(d\sigma/dt)$, where H is the Hubble parameter during inflation. This formula assumes that σ rolls down on its potential very slowly. In some cases, this fluctuation amplitude is about the same as adiabatic density fluctuations generated by a scalar field, ϕ, which drives inflation: $\delta\rho_\sigma/\rho_\sigma \sim \delta\rho_\phi/\rho_\phi \sim H^2/(d\phi/dt)$. This happens when both fluctuations are produced in a similar way, through the quantum-fluctuation production in inflation.

Even if $\delta\rho/\rho$ is similar to each other, the energy density, ρ, can be significantly different. Since ϕ drives inflation, its energy density, ρ_ϕ, dominates the total energy density of the universe during inflation: $\rho_\phi \gg \rho_\sigma$; thus, it gives $\delta\rho_\sigma \sim \delta\rho_\phi\,(\rho_\sigma/\rho_\phi) \ll \delta\rho_\phi$. Then, the density fluctuations generate the curvature perturbations, Φ. Since $\delta\rho_\sigma \ll \delta\rho_\phi$, σ makes negligible contribution to Φ compared with ϕ, i.e., $\delta\rho_\sigma$ does not generate the curvature perturbations, being an isocurvature mode. In this model, $\delta\rho_\sigma$ is Gaussian, as the quantum fluctuations have produced it linearly.

If σ moves fast, then the quantum fluctuations produce $\delta\rho_\sigma$ non-linearly; we have non-Gaussian density fluctuations. Linde and Mukhanov (1997) have proposed a massive-free field oscillating about its potential minimum as a possible non-Gaussian isocurvature-fluctuation production mech-

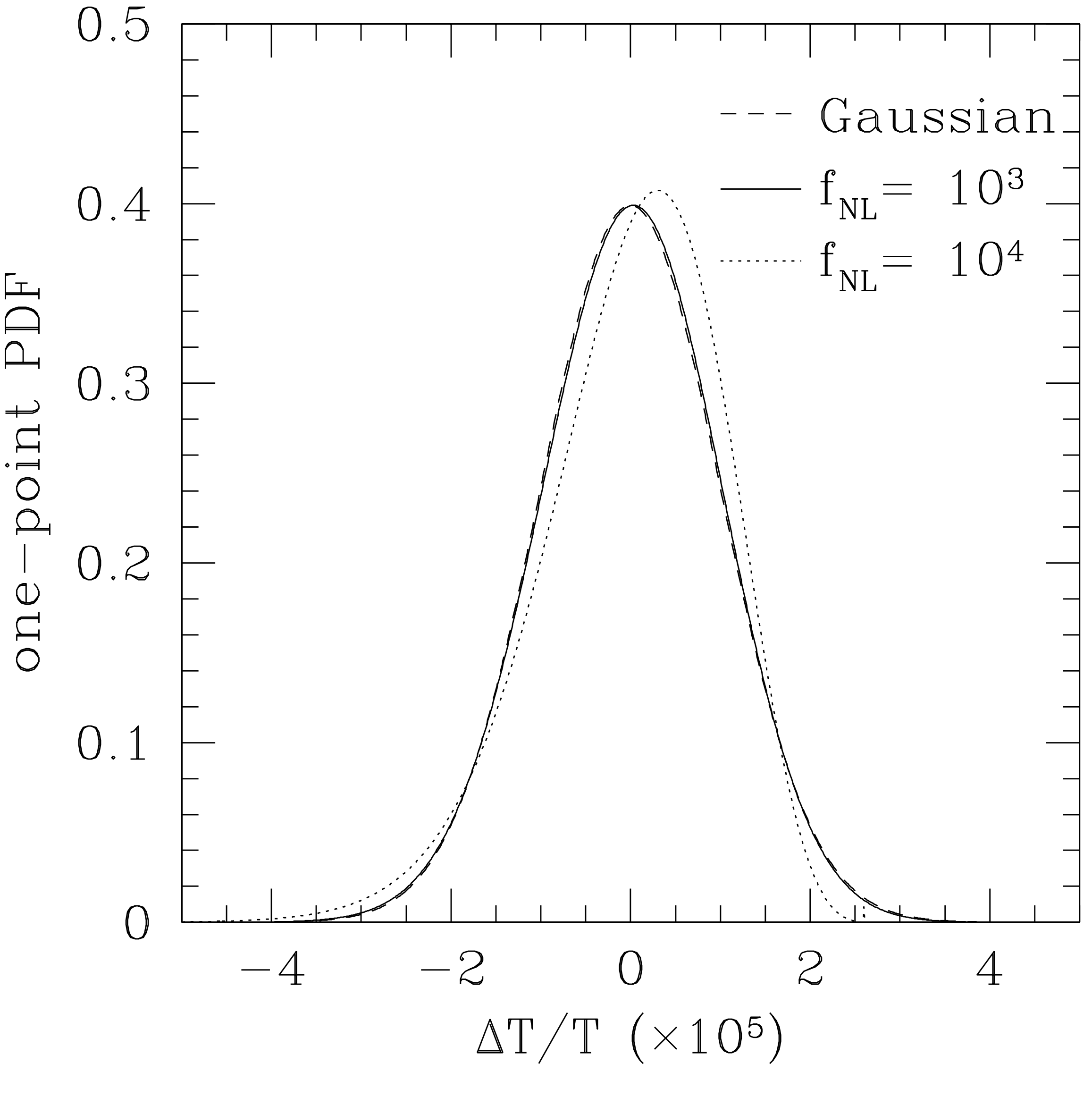

Figure 1.6: Adiabatic Non-Gaussianity: One-point p.d.f

One-point probability density distribution function (p.d.f) of the CMB anisotropy, $\Delta T/T$, comparing a Gaussian p.d.f with non-Gaussian p.d.f's of non-linear adiabatic fluctuations produced in inflation. The dashed line plots Gaussian distribution. The solid line plots non-Gaussian distribution for $f_{\rm NL} = 10^3$, the dotted line for $f_{\rm NL} = 10^4$. The larger $f_{\rm NL}$ is, the more negatively skewed p.d.f becomes. If $f_{\rm NL} < 0$, then p.d.f becomes positively skewed.

anism in inflation. The idea is as follows. When a field rolls down on a potential, $V(\sigma)$, very slowly, quantum fluctuations of σ, $\delta\sigma$, produce the energy density fluctuations of $\delta\rho_\sigma \sim (dV/d\sigma)\delta\sigma$; thus, $\delta\rho_\sigma$ is linear in $\delta\sigma$, being Gaussian. In contrast, when a field oscillates rapidly about $\sigma = 0$, there is no mean field; for example, a massive-free scalar field with a potential $V(\sigma) = m^2\sigma^2/2$ for $m \gtrsim H$ produces the density fluctuations of

$$\delta\rho_\sigma \sim m^2\sigma\delta\sigma + m^2(\delta\sigma)^2 = m^2(\delta\sigma)^2. \tag{1.7}$$

Here, $m \gtrsim H$ ensures that σ has rolled down to $\sigma = 0$ quickly, and oscillates. Hence, $\delta\rho_\sigma$ is *quadratic* in $\delta\sigma$, being non-Gaussian.

After the initial generation of isocurvature fluctuations, σ may produce the curvature perturbations through the evolution. If σ does not decay, or decays only very slowly, the energy density decreases as a^{-3}. On the other hand, the radiation energy density that is produced during the reheating phase by a decaying scalar field ϕ that has driven inflation decreases as a^{-4}; thus, at some point in the cosmic evolution, the σ-field energy density dominates the universe, producing the curvature perturbations,

$$\Phi(\mathbf{x}) = \eta^2(\mathbf{x}) - \left\langle \eta^2(\mathbf{x}) \right\rangle, \tag{1.8}$$

and hence the CMB anisotropies, $\Delta T/T \sim g_{\mathrm{T}}\Phi$. Here, η is a Gaussian fluctuation field which is related to $\delta\sigma$, and g_{T} is the isocurvature radiation transfer function. The Sachs–Wolfe effect gives $g_{\mathrm{T}} = -2$.

The CMB experiments show that isocurvature fluctuations do not contribute to the curvature perturbations very much; on the contrary, their contribution is negligible compared with adiabatic contribution. Figure 1.3 compares a prediction for the CMB angular power spectrum from adiabatic fluctuations with the data. The agreement is very good, and there is no need to invoke isocurvature fluctuations. Moreover, the isocurvature fluctuations predict a very different form of the power spectrum; thus, the data have excluded possibility of the isocurvature fluctuations dominating the observed CMB power spectrum at high significance.

Yet, there could exist isocurvature fluctuations in inflation. Generally speaking, if there are many scalar fields, there must exist isocurvature fluctuations. It is rather unusual to assume *only one* scalar field during inflation, for currently viable theories of the high energy particle physics predict existence of many kinds of scalar fields in a very high energy regime. There is, however, little hope to detect their signatures in the CMB power spectrum, as they are so weak compared with adiabatic fluctuations. Instead, searching for non-Gaussian signals in CMB is a promising strategy to look for some of those isocurvature fluctuations which are generally much more non-Gaussian than the adiabatic fluctuations.

Since $\Delta T/T$ is quadratic in a Gaussian variable, one-point p.d.f of $\Delta T/T$ is the χ^2 distribution with one degree of freedom. Figure 1.7 plots the one-point p.d.f of the isocurvature model (solid line) in comparison with Gaussian p.d.f (dashed line). The predicted p.d.f is highly non-Gaussian. If we assume the isocurvature CMB fluctuations dominating the universe, then the predicted non-Gaussian p.d.f may look too non-Gaussian to be consistent with observations; however, the *COBE* DMR data do not exclude this model on the basis of the non-Gaussianity because of the large beam-smoothing effect (Novikov et al., 2000). The bigger the beam is, the closer the smoothed χ^2 distribution is to Gaussian distribution (Novikov et al., 2000). The CMB experiments probing much smaller angular scales than DMR will test the isocurvature non-Gaussian models.

While we do not explore the isocurvature fluctuations so extensively, we present in appendix C an analytic prediction for the CMB angular bispectrum generated from the isocurvature fluctuations that we have described in this section. This formula may be used to fit the measured bispectrum; by doing so, we can constrain the model independently of the angular power spectrum. Although the one-point p.d.f of the isocurvature fluctuations is very similar to Gaussian distribution for large-beam CMB experiments, the bispectrum may still be powerful enough to detect the non-Gaussian signals.

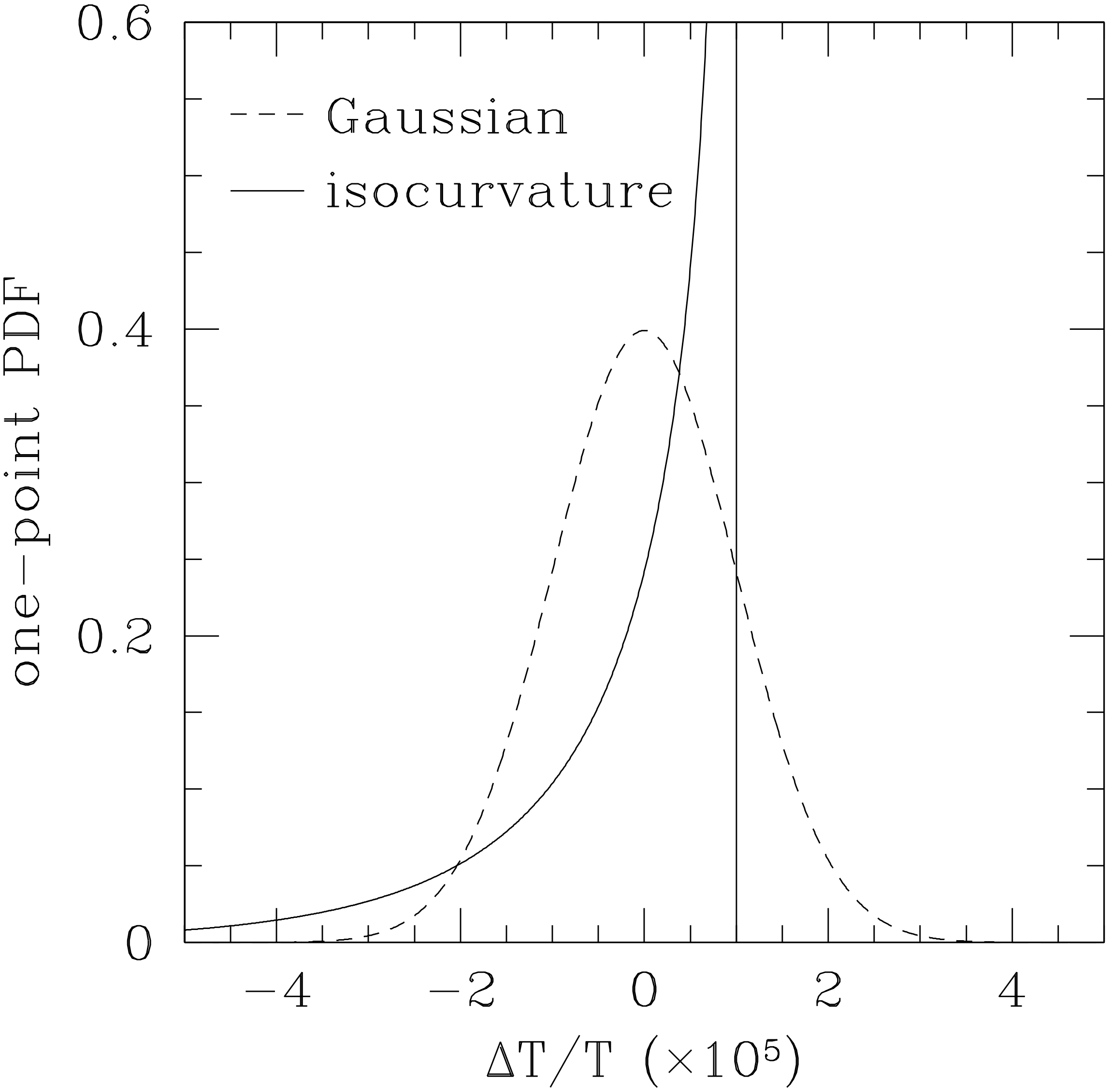

Figure 1.7: Isocurvature Non-Gaussianity: One-point p.d.f

One-point probability density distribution function (p.d.f) of the CMB temperature anisotropy, $\Delta T/T$, comparing a Gaussian p.d.f with a non-Gaussian p.d.f of isocurvature fluctuations produced in inflation (Linde and Mukhanov, 1997). The dashed line plots Gaussian distribution, while the solid line plots the non-Gaussian distribution. Note that we have assumed no beam smoothing; the large beam smoothing makes the non-Gaussian distribution similar to the Gaussian distribution (Novikov et al., 2000).